Chromosomal Microarray Analysis in the Era of Optical Genome Mapping: Clinical Implications in Detecting Copy-Neutral Events

Alexander R. Marr , Patrick R. Gonzales , Shivani Golem *

Posted Date: 8 May 2026

doi: 10.20944/preprints202605.0494.v1

Keywords: cytogenetics; optical genome mapping; chromosomal microarray; copy-neutral loss of heterozygosity; karyotype; genomics

 doi:10.20944/preprints202605.0494.v1

Article

Chromosomal Microarray Analysis in the Era of Optical Genome Mapping: Clinical Implications in Detecting Copy-Neutral Events

Alexander R. Marr, Patrick R. Gonzales and Shivani Golem *

Department of Pathology and Laboratory Medicine, University of Kansas Medical Center, Kansas City, KS 66160, USA

* Correspondence: sgolem@kumc.edu

Simple Summary

Cytogenetic testing plays a key role in diagnosis and treatment selection for many blood cancers. Several laboratory methods are currently used, each with different strengths and limitations. A new technology called optical genome mapping has the potential to replace older methods by providing a comprehensive and streamlined view of complex genetic changes. However, it may miss smaller but clinically important alterations that can affect treatment decisions. In our study, we reviewed patient cases performed at our institution to determine how frequently these small changes occur and whether they remain clinically important. We found many of these alterations to involve key cancer genes and often occur alongside other mutations that influence disease behavior. Our findings suggest that combining multiple testing methods provides the most complete and reliable genetic assessment for cancer patients until technology improves.

Abstract

Background/Objectives: Chromosomal microarray analysis (CMA) is an essential tool in modern cytogenetics for detecting copy number alterations and copy-neutral loss of heterozygosity (CN-LOH). As optical genome mapping (OGM) emerges as a potential replacement for traditional cytogenetic methods, the extent to which CMA remains necessary in routine diagnostic workflows remains to be elucidated. **Methods**: We retrospectively reviewed 53 primary neoplastic cases in which CMA identified one or more CN-LOH events. Event size, genomic content, and correlation with next-generation sequencing (NGS) findings were assessed. A separate cohort of newly diagnosed B-cell acute lymphoblastic leukemia (B-ALL) was analyzed to evaluate disease-specific CN-LOH frequency. **Results**: Nearly half of CN-LOH events detected were <25 Mb, below the current detection threshold of OGM. Many encompassed clinically relevant genes, including *FLT3, JAK2, TET2, TP53,* and *RUNX1*. Additionally, two-thirds of cases harbored pathogenic or likely pathogenic variants by NGS within the corresponding CN-LOH regions, further underscoring the clinical value of detecting these copy-neutral events. In contrast, CN-LOH was uncommon in B-ALL, and most alterations identified by CMA would be detectable by OGM. Many of these patients also harbored complex structural rearrangements that required multiple conventional assays for full characterization; these could be resolved by OGM in a single analysis. **Conclusions:** Our findings indicate that although OGM excels at resolving complex structural variants, CMA remains essential for detecting copy-neutral events. Until OGM achieves improved sensitivity for CN-LOH, an integrated approach utilizing conventional cytogenetics, CMA, NGS, and OGM provides the most reliable framework for comprehensive genomic assessment across cancer types.

Keywords: cytogenetics; optical genome mapping; chromosomal microarray; copy-neutral loss of heterozygosity; karyotype; genomics

 doi:10.20944/preprints202605.0494.v1

1. Introduction

Classical cytogenetics has served as the cornerstone for diagnostic and prognostic classification of cancers for decades but remains limited by relatively low-resolution technologies and high labor intensity[1,2]. Identification of hallmark chromosomal abnormalities is integral for clinical diagnosis, risk stratification, and therapeutic decision-making, particularly in hematologic malignancies[3,4]. Technological advances such as chromosomal microarray (CMA) have broadened the scope of cytogenetic testing, enabling genome-wide detection of copy number (CN) variants and copy-neutral events, such as copy-neutral loss-of-heterozygosity (CN-LOH)[5,6]. Several clinically significant regions of CN-LOH have been identified on 4q, 9p, 13q, and 17p, among others, and their accurate recognition has become essential for routine testing and prognostic stratification [5,7].

Current gold-standard practice in cytogenetics laboratories relies on a combination of conventional karyotyping and fluorescence in-situ hybridization (FISH)[1,3]. Identification of recurrent abnormalities, such as deletions of 5q and 7q in acute myeloid leukemia (AML), provides important prognostic information to guide treatment selection[4]. However, both techniques have limitations. For example, FISH is limited to predefined genomic regions, while karyotyping is technically challenging, time-consuming, and constrained by low-resolution capabilities[7–9]. These challenges have driven the need for high-resolution, genome-wide solutions.

CMA offers a genome-wide, high-resolution capability for detecting submicroscopic CN changes and regions of allelic imbalance[6]. Importantly, CMA can also detect small CN-LOH events within clinically significant regions, aiding prognostic stratification[10]. Currently, CMA has become an established complementary method to conventional karyotyping and FISH for both neoplastic and constitutional testing[3,6,10]. However, its inability to detect balanced rearrangements necessitates the use of additional molecular methods.

The limitations of current cytogenetic techniques have created demand for comprehensive, streamlined technology. Optical Genome Mapping (OGM) has emerged as such a platform, offering direct, high-resolution imaging of ultra-high-molecular-weight DNA to visualize structural variants [11,12]. Often described as "next-generation cytogenetics," OGM is increasingly adopted by clinical laboratories for the characterization of structural variants in cancer[11–15]. Multiple studies have highlighted OGM's key strengths, including excellent breakpoint resolution and high sensitivity for variants >500 bp in size[16–18]. Further, complex karyotypes can be easily resolved, and workflows are streamlined compared to conventional karyotyping. These features position OGM as an attractive alternative to traditional techniques, promising to consolidate multiple workflows into a single assay.

Despite these advantages, OGM's sensitivity for CN-LOH detection is a key limitation and could be particularly problematic in disorders where biallelic inactivation is significant[15,19]. For example, homozygosity for driver mutations in genes such as *JAK2*, *CBL*, *TET2*, or *TP53* can be essential findings for clinical management[20–23]. While OGM excels at characterization of structural rearrangements, its lack of allelic resolution represents a critical diagnostic and prognostic constraint. Accurate detection of CN-LOH remains vital for comprehensive genomic interpretation and optimal clinical management in the age of precision medicine.

As laboratories transition toward OGM adoption, the question remains whether CMA should still have a place in modern workflows. To address this, we retrospectively analyzed 53 neoplastic CMA cases collected at the University of Kansas Health System (TUKHS) that included at least one CN-LOH event. Our findings demonstrate that, although OGM would enhance structural variant detection, clinically significant focal copy-neutral events may go undetected. These results highlight the continued importance of performing CMA as a complementary modality in the ascendant era of OGM.

2. Materials and Methods

 doi:10.20944/preprints202605.0494.v1

2.1. Patient Samples

327 patients with hematological malignancies at TUKHS from 2025 were included in the study. The cancer diagnosis was performed on blood or bone marrow by morphological and flow cytometry evaluations, as a standard clinical practice. Next-generation sequencing (NGS) using the QIAseq Targeted DNA Human Myeloid Neoplasms 141 gene Panel was also performed. Clinical significance of NGS variants was reported as per published guidelines [24]. The results of these evaluations were retrospectively reviewed from the patient's medical records.

Karyotyping, FISH, and Neoplastic CMA were performed at TUKHS Cytogenetics Laboratory. No patients were excluded. All testing was performed as part of routine clinical care. The retrospective review was approved by an institutional review board (Study ID: STUDY00160638, approved on 20th June 2024).

2.2. Karyotyping and FISH Analysis

Conventional karyotyping and FISH analyses were performed on cultured peripheral blood or bone marrow specimens using standard cytogenetic protocols. A minimum of 20 metaphases were evaluated for each case. FISH testing included acute myeloid leukemia (AML) FISH probes *RUNX1T1*::*RUNX1*, *KMT2A*, *PML*::*RARA*, *MYC*, and 7q probes from Abbott, and 5q, *CBFB*::*MYH11*, *MECOM*, and *PML*::*RARA* from Cytocell and *TP53* from MetaSystems. B-cell acute lymphoblastic leukemia (B-ALL) -associated FISH probes included *BCR*::*ABL*1, *KMT2A*, *CDKN2A*, *IGH*, and *MYC* from Abbott, *ETV6*::*RUNX1*, *ABL2*, *PDGFRB*, *JAK2*, *EPOR*, *CRLF2*, and *P2RY8* from Cytocell, and *IKZF1* from Empire Genomics. 200~500 interphase cells were scored for FISH. Chromosome and FISH analysis was performed utilizing Cytovision Software (Leica). Results were interpreted and reported using the International System for Human Cytogenomic Nomenclature (ISCN 2024).

2.3. DNA Extraction

Genomic DNA was extracted from peripheral blood or bone marrow using the QIAamp DNA Blood Mini Kit (Qiagen) according to the manufacturer's instructions. DNA was quantified by Qubit fluorometry. At least 200 ng of total DNA was utilized for CMA.

2.4. Chromosomal Microarray

Microarray-based chromosome analysis was performed using the iScan System with the Global Diversity Array-8 (GDACyto) v1.0 Array BeadChip (Illumina). Criteria for designating reportable aberrations include gains or losses larger than 50 kb involving clinically significant cancer genes, gains >2 Mb, and losses >1 Mb outside known clinically significant oncology regions spanning at least one annotated RefSeq gene. Smaller aberrations are reported only if the regions are likely to be clinically significant. Copy-neutral loss of heterozygosity (CN-LOH) are reported when the region exceeds 3 Mb. CMA analysis and visualization were performed using NxClinical 6.2 (Bionano).

All NGS and CMA findings are annotated using the human genome reference build GRCh37/hg19.

2.5. Statistics

Descriptive statistics, including frequencies, median values, and distribution counts, were generated in Microsoft Excel or R. Figures were generated using R (v4.5.1).

3. Results

3.1. Assessing the Impact of CN-LOH Events in Routine Neoplastic Testing

TUKHS Cytogenetics Laboratory performed neoplastic CMA on 327 patients aged 18 to 92 years in 2025. 184 patients were male, 142 were female, and one identified as other. Among this cohort,

 doi:10.20944/preprints202605.0494.v1

53 patients were selected who demonstrated at least one CN-LOH event, and retrospective analysis was performed to evaluate the prospective clinical value OGM could have provided in lieu of CMA. The average patient age was 64 years, with 28 male and 25 female cases. The full demographic, cytogenetic, and molecular results of our patient cohort are summarized in **Table 1**. These cases served as the foundation of our comparative analysis of CMA and potential OGM coverage.

Table 1. Patient cohort demographic, cytogenetic, and molecular characteristics.

Patient	Age	Diagnosis	CMA Events	Size of LOH:	Karyotype	FISH	NGS
1	56	Myelofibrosis	CN-LOH: 9p24.3p21.3(14326_20760511)x2 mos hmz CN-LOH: 9p21.3p21.1(20760922_28181085)x2 mos hmz CN Loss: 3q26.31(171567390_173777284)x1~2	20.7 Mb ; 7.4 Mb	46,XY[20]	N/A	***JAK2*** p.V617F, c.1849G>T *TNFRSF13B* p.I87N, c.260T>A
2	77	Essential Thrombocytosis (ET)	CN-LOH: 9p24.3p21.1(14326_28208071)x2 mos hmz	28.2 Mb	46,XY[20]	N/A	*IDH2* p.R140Q, c.419G>A ***JAK2*** p.V617F, c.1849G>T *SRSF2* p.P95H, c.284C.A *TET2* p.Q461*, c.1381C>T
3	46	Myelofibrosis	CN-LOH: 9p24.3p21.1(14326_28177028)x2 mos hmz CN-LOH: 9p21.1p13.3(28215694_34098370)x2 mos hmz	28.2 Mb ; 5.9 Mb	46,XX[20]	N/A	***JAK2*** p.V617F, c.1849G>T
4	45	MDS	CN-LOH: 4q32.1q35.2(78822339_191039443)x2 mos hmz	112.2 Mb	46,XY[20]	N/A	*JAK2* p.V617F, c.1849G>T*NF1* p.S302N, c.905G>A*SF3B1* p.R625G, c.1873C>G***TET2*** p.Y1345*, c.4035T>A*CUX1* p.P1168Nfs*8, c.3501_3504del*PHF6* p.C17Mfs*5, c.48dup
5	76	CMML	CN-LOH: 4q21.22q35.2(83649829_191039443)x2 hmz CN-LOH: 9p24.3p21.3(14326_25040147)x2 mos hmz CN-LOH: 9p21.3p21.1(25040148_28186091)x2 mos hmz CN-LOH:	107.4 Mb ; 25.0 Mb ; 3.1 Mb ; 11.1 Mb	46,XX[20]	N/A	***JAK2*** p.V617F, c.1849G>T *SRSF2* p.P96L, c.287C>T ***TET2*** p.S1303Afs*69, c.3907del

 doi:10.20944/preprints202605.0494.v1

			9p21.1p13.1(28186092_39239372)x2 mos hmz				
6	78	MDS	CN-LOH: 7q11.23q36.3(75603594_159138663)x2 hmz	83.5 Mb	46,XX[20]	N/A	*ASXL1* p.P808Lfs*10, c.2423del***EZH2*** c.2196-1G>C *PTPN11* p.Q79R, c.236A>G*RUNX1* c.497_508+7del*TET2* p.W1847*, c.5540G>A
7	75	Myelofibrosis	CN-LOH: 9p24.3p22.3(14326_15468633)x2 mos hmz CN-LOH: 9p22.3p13.3(15468706_34387524)x2 mos hmz	15.5 Mb ; 18.9 Mb	46,XX[20]	N/A	***JAK2*** p.V617F, c.1849G>T
8	75	MDS	CN Gain: 5q12.3q13.2(66303158_71398049)x2~3CN Loss: 5q12.3(65868766_66300298)x1~2CN Gain: 5q13.2q13.3(71398418_74530657)x3CN Gain: 5q13.3(75096560_75681806)x2~3CN Gain: 5q13.3(74530658_75096559)x2~3CN Loss: 5q13.3q14.2(75690122_82633950)x1~2CN Gain: 5q14.2(82633951_82671099)x2~3CN Loss: 5q14.2q35.1(82671100_172787322)x1~2CN Gain: 5q35.1q35.2(172790755_173859463)x3CN Gain: 5q35.2(173862444_175554718)x2~3CN Loss: 5q35.2q35.3(175554719_180709213)x1~2CN Gain: 6p22.2(25697364_26027479)x3CN Gain: 6p24.3(7101019_7179975)x2~3CN Loss: 6p25.3p24.3(149609_7101018)x1~2CN Loss: 6p24.3p22.2(7179976_25694491)x1~2CN Loss: 6p22.2(26030492_26624822)x1~2CN Gain: 6p22.2p21.31(26629404_34263743)x3CN Gain: 6p21.31p21.2(36020459_38318789)x3CN Loss: 6p21.1p12.3(44233451_47303071)x1~2CN Gain:	20.0 Mb	46,XY,psudic(6;5)(5pter->5q11.2::?::6p21.3->6qter),+8[19]/46,XY[1]	nuc ish(D5S630x2,EGR1x1)[118/200], (RUNX1T1x3,RUNX1x2)[113/200]	***TP53*** p.Y234D, c.700T>G

 doi:10.20944/preprints202605.0494.v1

			(8)x2~3CN-LOH: 17p13.3p11.2(1389_20011659)x2 mos hmz				
9	53	AML	CN-LOH: 21q11.2q22.3(14343435_48096251)x2 mos hmz	33.8 Mb	93,XXYY,+4[3]/46,XY[17]	nuc ish (GOLIM4/EGFEM1P, MECOM,LRRC34)x4[42/200],(TP53,NF1)x4[41/200],(MYH11,CBFB)x4[31/200],(KMT2Ax4)[27/200],(RUNX1T1,RUNX1)x4[25/200]	*IDH1* p.R132C, c.394C>T ***RUNX1*** p.Q264Efs*?, c.790_791del *PHF6* p.Y124*, c.372C>A *SUZ12* c.505+1G>A
10	72	Myelofibrosis	CN-LOH: 9p24.3p24.1(14326_5969307)x2 mos hmz	6.0 Mb	46,XY[20]	N/A	***JAK2*** p.V617F, c.1849G>T*TP53* p.C242Afs*5, c.723del*U2AF1* p.Q157P, c.470A>C*PDGFRA* p.V159I, c.475G>A*CUX1* p.R147*, c.439C>T
11	56	Myelofibrosis	CN-LOH: 9p24.3p11.2(14326_47204861)x2 mos hmz	47.2 Mb	46,XY[20]	N/A	***JAK2*** p.V617F, c.1849G>T *CBL* p.N754D, c.2260A>G *EZH2* p.R288*, c.862C>T *GATA2* p.T387_E391delinsK, c.1160_1171del
12	66	MDS/MPN	CN-LOH: 11p15.5p11.2(180184_47788140)x2 hmz CN-LOH: 18q12.2q23(33047750_78014582)x2 hmz	47.6 Mb ; 45.0 Mb	46,XY[20]	N/A	*PTPN11* p.G60V, c.179G>T ***SETBP1*** p.D868N, c.2602G>A *DNMT3A* p.R882H, c.2645G>A
13	79	AML	CN-LOH: 10q22.1q25.1(72509080_108727129)x2 mos hmz	36.2 Mb	46,XY[20]	nuc ish (GOLIM4/EGFEM1P, MECOM,LRRC34)x2[200],(RUNX1T1,RUNX1)x2[200],(KMT2Ax2)[200],(M	*ASXL1* p.Q592*, c.1774C>T*IDH2* p.R140Q, c.419G>A*SRSF2* p.P95H, c.284C>A*PHF6* p.C28Mfs*8, c.81dup*TET2*

 doi:10.20944/preprints202605.0494.v1

						YH11,CBFB)x2[200],(TP53,NF1)x2[200]	p.Q904*, c.2710C>T
14	70	MDS/MPN	CN-LOH: 9p24.3p21.1(14326_30464776)x2 mos hmz	30.5 Mb	46,XX[20]	N/A	***JAK2*** p.V617F, c.1849G>T *SF3B1* p.K666R, c.1997A>G *DDX41* p.M1I, c.3G>A
15	20	T-ALL	CN Gain: (8)x2~3 CN-LOH: (9)x2 mos hmz	141.2 Mb	46,XX[13]	nuc ish (CDKN2A, CEP9)x2[200]	***NOTCH1*** p.P2514Rfs*, c.7541_7542del ***NOTCH1*** p.L1600P, c.4799T>C
16	67	AML	CN-LOH: 21q11.2q22.3(15695598_48129895)x2 hmz	32.4 Mb	46,XY[20]	nuc ish (GOLIM4/EGFEM1P, MECOM,LRRC34)x2[200],(RUNX1T1,RUNX1)x2[200],(KMT2Ax2)[200],(MYH11,CBFB)x2[200],(TP53,NF1)x2[200]	*DNMT3A* p.R882H, c.2645G>A*IDH2* p.R140Q, c.419G>A***RUNX1*** p.L98Sfs*24, c.292del*JAK2* p.V617F, c.1849G>T*SRSF2* p.P95H, c.284C>A
17	75	AML	Loss: 3q21.3q22.1(128391789_133052381)x1~2 Loss: 5q31.1q35.3(133745634_178977650)x1~2 Loss: (7)x1~2 CN-LOH: 9p24.3p23(14326_12903066)x2 mos hmz CN-LOH: 17p13.3p13.1(1389_8286478)x2 mos hmz	12.89 Mb ; 8.29 Mb	45,X,dic(Y;18)(p11.3;p11.3),add(5)(q11.2)[cp11]/45,XY,del(3)(q12q26.1),add(5)(q13),-7[3]/46,XY[6]	nuc ish (D7Z1, D7S486)x1[83/200],(D5S630x2,EGR1x1)[45/200], (GOLIM4/EGFEM1Px3,MECOMx2,LRRC34x2)(GOLIM4/EGFEM1P sep GOLIM4/EGFEM1P/MECOM sep LRRC34)x1[70/200]/(GOLIM4/EGFEM1Px3,MECOMx2,LRRC34x2)(GOLIM4/EGFEM1P sep	*ASXL1* p.E635Rfs*15, c.1900_1922del *ETV6* p.V146Sfs*63, c.436del ***JAK2*** p.V617F, c.1849G>T *U2AF1* p.Q157P, c.470A>C

 doi:10.20944/preprints202605.0494.v1

						GOLIM4/EGFEM1P/MECOM/LRRC34)x1[21/200]	
18		AML	CN-LOH: 21q21.1q22.12(17593180_35853470)x2 mos hmzCN-LOH: 21q22.12(35853471_36103063)x2 mos hmzCN-LOH: 21q22.12(36103064_36224144)x2 mos hmzCN-LOH: 21q22.12(36224145_37431159)x2 mos hmzCN-LOH: 21q22.12q22.3(37431160_48129895)x2 mos hmz	18.3 Mb ; 0.25 Mb ; 0.12 Mb ; 1.2 Mb ; 10.7 Mb	46,XY,t(8;9)(p22;p24)?c[20]//	N/A	*ASXL1* p.A627Gfs*8, c.1879dup***RUNX1*** p.P426Qfs*?, c.1277delinsA *APTPN11* p.D61Y, c.181G>T*KMT2C* p.R1279Qfs*23, c.3835_3838del
19	20	AML	CN-LOH: 11q14.1q25(82922310_134945709)x2 mos hmz CN Gain: 11q23.3(118332913_118357325)x3	52.0 Mb	46,XX[20]	nuc ish (GOLIM4/EGFEM1P,MECOM,LRC34)x2[200],(D5S630,EGR1)x2[200],(D7Z1,D7S486)x2[200](RUNX1T1,RUNX1)x2[200],(KMT2Ax2)[200],(MYH11,CBFB)x2[200],(TP53,NF1)x2[200]	*WT1* p.T382Kfs*8, c.1145_1147delinsAAGG *WT1* p.R374Gfs*7, c.1119_1120insGG
20	69	Myelofibrosis	CN-LOH: 1p36.33p33(49554_47656596)x2 mos hmzCN-LOH: 1p33p21.1(47657141_106663742)x2 mos hmzCN Loss: 13q13.3q21.1(38679113_56493483)x1~2	47.61 Mb ; 59.01 Mb	46,XY[20]	N/A	*ASXL1* p.G646Wfs*12, c.1934dup***MPL*** p.W515A, c.1543_1544delinsGC
21	63	AML	CN Loss: 9q21.11q21.33(70971846_88790268)x1 CN-LOH: 13q12.13q34(25795201)115106996)x2 hmz	89.3 Mb	46,XX[20]	nuc ish (D5S630,EGR1)x2[500],(PDGFRBx2)[500],(TP53,NF1)x2[500]	*DNMT3A* p.R882C, c.2644C>T ***FLT3*** p.P606_R607insKREYEYDLKWEFP, c.1819_1820insAAAGAGAAATATGAATATGATCTCAAATGGGAGTTTCCAA

 doi:10.20944/preprints202605.0494.v1

22	51	Polycythemia vera (PV)	CN-LOH: 9p24.3p13.1(14326_38777298)x2 mos hmz	38.76 Mb	46,XX[20]	N/A	***JAK2*** p.V617F, c.1849G>T
23	83	MDS	CN Loss: 4q24(105823175_106397864)x1 CN-LOH: 12p13.33p13.31(83247_8860001)x2 mos hmz CN-LOH: 12q13.2q14.1(56349167_62288780)x2 mos hmz CN-LOH: 12q14.1q24.33(62288781_133838353)x2 mos hmz	8.8 Mb ; 5.9 Mb ; 71.5 Mb	45,X,-Y[20]	N/A	*RUNX1* p.S141L, c.422C>T *PHF6* p.Y301*, c.902dup *PHF6* p.I314T, c.941T>C *PHF6* p.R319*, c.955C>T
24	69	MPN	CN-LOH: 9p24.3p21.3(14326_20614991)x2 mos hmz	20.6 Mb	47,XX,+8[3]/46,XX[17]	N/A	***JAK2*** p.V617F, c.1849G>T
25	66	Polycythemia vera (PV)	CN-LOH: 9p24.3p13.3(14326_35869953)x2 mos hmz	35.9 Mb	46,XX[20]	N/A	***JAK2*** p.V617F, c.1849G>T
26	56	AML	CN-LOH: 13q12.11q35(20356854_115106996)x2 mos hmz	94.75 Mb	46,XX[20]	nuc ish (RUNX1T1,RUNX1)x2[200],(KMT2Ax2)[200],(PML,RARA)x2[200],(MYH11,CBFB)x2[200],(TP53,NF1)x2[200]	*DNMT3A* p.R882C, c.2644C>T ***FLT3*** p.D593_W603dup, c.1779_1811dup *NPM1* p.W288Cfs*?, c.860_863dup *TET2* p.L1212*, c.3635T>A *TET2* p.Y1255*, c.3764dup *SF3B1* p.K700E, c.2098A>G
27	63	Myelodysplastic neoplasm	CN-LOH: 4q22.1q35.2(91997582_191039443)x2 mos hmz	99.04 Mb	46,XX[20]	N/A	*DNMT3A* p.W860*, c.2580G>A ***TET2*** p.Y1245Lfs*22, c.3732_3733del
28	71	Essential Thrombocytosis (ET)	CN-LOH: 14q32.13q32.33(95803335_107289356)x2 mos hmz	11.5 Mb	46,XX[20]	N/A	*CALR* p.L367Tfs*, c.1099_1150del
29	56	Polycythemia vera (PV)	CN-LOH: 9p24.3p13.3(14326_36203718)x2 mos hmz	36.2 Mb	46,XX[20]	N/A	*ASXL1* p.G646Wfs*12, c.1934dup*DNMT3A* p.R736C, c.2206C>T*IDH1* p.R132H,

 doi:10.20944/preprints202605.0494.v1

30	78	MDS	CN-LOH: 7q11.23q36.3(73589034_159122659)x2 hmz	85.53 Mb	46,XX[20]	N/A	c.395G>A***JAK2*** p.V617F, c.1849G>T*NBN* p.E658Dfs*6, c.1974del *ASXL1* p.P808Lfs*10, c.2423del ***EZH2*** c.2196-1G>C *PTPN11* p.Q79R, c.236A>G *TET2* p.W1847*, c.5540G>A
31	38	B-cell ALL	CN Gain: 1q21.1q44(145208887_249212725)x2~3CN Loss: 5q35.2q35.3(175882256_177046240)x1~2CN Gain: 8p23.3p22(30600_17880616)x2~3CN Loss: 8q24.21(128786292_128982046)x1~2CN-LOH: 9p24.1p13.1(5062826_38919047)x2 mos hmzCN Loss: 9p24.3p24.1(14326_5061562)x1~2CN Loss: 22q11.22(22697843_232376744)x1	33.9 Mb	46,XY,+1,t(8;22)(q24.1;q11.2),add(9)(p22)x2,dic(1;14)(p11;p11.2)[cp3]/46,XY[17]	nuc ish (3'JAK2x2, 5'JAK2x1)[40/200]	***CDKN2A*** c.156_193+1del
32	66	Myelofibrosis	CN-LOH: 9p24.3p13.3(14326_33870457)x2 mos hmz	33.9 Mb	47,XX,+8[6]/46,XX[14]	N/A	*DNMT3A* p.L738dup, c.2211_2213dup ***JAK2*** p.V617F, c.1849G>T *KMT2C* p.Q968*, c.2902C>T *PMS2* p.T728Afs*7, c.2182_2184delinsG
33	64	Polycythemia vera (PV)	CN Gain: 1q21.1q44(146074350_249212725)x2~3CN-LOH: 9p24.3p11.2(14326_47204861)x2 mos hmzCN Loss: 18q21.2q23(51583029_78014582)x1~2	47.2 Mb	46,XY,add(1)(p36.1)[6]/46,XY,der(18)t(1;18)(q12;q21.1)[6]/46,XY,der(15)t(1;15)(q12;p11.2)[2]/46,XY[6]	N/A	*ASXL1* p.T880lfs*6, c.2639del***JAK2*** p.V617F, c.1849G>T
34	61	MDS	CN Gain: (X)x2 CN LOH: Xp21.2q22.3(29652995_107217256)x2 hmz CN LOH: Xq27.3q28(145010330_15492	77.56 Mb ; 9.91 Mb	48,XXYc,+8[4]/47,XXYc[16]	N/A	***BCOR*** p.K699Gfs*14, c.2094_2101delinsT

 doi:10.20944/preprints202605.0494.v1

			2555)x2 hmz CN Gain: (8)x2~3 CN-LOH: 2p24.1p23.1(19552065_31154 708)CN-LOH: 8q12.3q13.3(65828731_72260 121)CN-LOH: 11q22.1q24.2(98453463_1239 24760)CN-LOH: 14q32.2q32.31(99664084_101 893204)CN-LOH: 16q12.2q23.2(55509628_8018 8851)CN-LOH: 17q22q25.1(55345474_74591 725)CN-LOH: 19p13.11p11(17130401_2459 4907)CN-LOH: 19q11q13.2(27733480_40336 910)CN-LOH: 20q12q13.12(40570082_4523 4542)CN-LOH: 20q13.2q13.33(51902758_629 54925)CN-LOH: 22q13.1q13.2(40132529_4279 3122)				
35	70	MDS		11.6 Mb ; 6.4 Mb ; 25.5 Mb ; 2.2 Mb ; 24.7 Mb; 19.2 Mb ; 7.5 Mb ; 12.6 Mb ; 4.7 Mb ; 11.1 Mb ; 2.7 Mb	45,X,-Y[8]/46,XY[20]	N/A	Inconclusive
36	89	AML	CN Gain: (8)x2~3 CN-LOH: 9p24.3p13.3(1_34220621)x2 mos hmz CN Gain: (19)x2~3 CN Gain: (21)x2~3	34.2 Mb	47,XY,+19[cp2]/48,sl,+8[cp16]/49,sdl,+21[cp2]	nuc ish (RUNX1T1,RUNX1)x2[200],(KMT2Ax2)[200],(PML,RARA)x2[200],(MYH11,CBFB)x2[200],(TP53,NF1)x2[200]	*SRSF2* p.P95R, c.284C>G *SETBP1* p.D868N, c.2602G>A *TET2* p.R571Vfs*9, c.1711del
37	88	AML	CN-LOH: 1p36.33p13.2(49554_1151679 39)x2 hmzCN-LOH: 9p24.3p21.1(14326_28223556)x2 mos hmzCN-LOH: 9p21.1p13.3(28223906_33506 670)x2 mos hmzCN-LOH: 9p13.3p13.2(33518282_37235 170)x2 mos hmz	115.1 Mb ; 28.2 Mb ; 5.3 Mb ; 3.7 Mb	46,XX[20]	N/A	*GATA2* p.L359V, c.1075T>G***JAK2*** p.V617F, c.1849G>T*NRAS* p.G12D, c.35G>A*SF3B1* p.K666N, c.1998G>C*TET2* p.G1288D, c.3863G>A*TET2* p.Q1813Pfs*9, c.5437dup
38	85	MDS	CN Gain: (8)x2~3 CN-LOH: 14q21.1q32.33(43421852_107 289356)x2 mos hmz	63.9 Mb	47,XX,+8[7]/46,XX[13]	N/A	*SF3B1* p.K700E, c.2098A>G *DNMT3A* p.R882H, c.2645G>A
39	74	MPN	CN-LOH: 9p24.3p22.3(14616_15513161	15.5 Mb ; 18.7 Mb	46,XX[20]	N/A	***JAK2*** p.V617F, c.1849G>T

 doi:10.20944/preprints202605.0494.v1

			)x2 hmz CN-LOH: 9p22.3p13.3(15513162_34256984)x2 mos hmz				
40	75	MDS	CN Loss: 21q22.12(36171307_36252056)x1~2 CN-LOH: 21q22.13q22.3(38695572_48129895)x2 mos hmz	9.43 Mb	46,XY[20]	N/A	*BCOR* o.E1236Kfs*2, c.3706del *KRAS* p.A146P, c.436G>C *KRAS* p.A146T, c.436G>A ***U2AF1*** p.S34F, c.101C>T *WT1* p.A387Vfs*4, c.1156_1159dup
41	66	MDS	CN Loss: 3p14.2(60280743_60611316)x1CN Gain: (8)x2~3CN-LOH: 21q21.1q22.3(16841195_480966251)x2 mos hmz	31.26 Mb	46,XY[20]	N/A	*BCOR* p.E1337Kfs*32, c.4009del*SRSF2* p.P95_R102del, c.284_307del*STAG2* p.M139Afs*4, c.415_416del*STAG2* p.K551Nfs*8, c.1653_1656delinsTC*PHF6* p.R319*, c.955C>T *ASXL1* p.G646Wfs*12, c.1934dup
42	68	MDS	CN-LOH: 7q32.1q36.3(127988628_159138663)x2 mos hmz CN Gain: (8)x2~3	31.2 Mb	47,XX,+8[20]	N/A	*ETV6* p.Q219Sfs*25, c.654dup *GATA2* p.P385L, c.1154C>T *DNMT3A* p.R882H, c.2645G>A *IDH1* p.R132H, c.395G>A *NPM1* p.W288Cfs*?, c.860_863dup *PTPN11* p.I282V, c.844A>G *PRF1* p.C73R, c.217T>C
43	62	AML	CN-LOH: 22q11.1q13.33(16052962_51224267)x2 mos hmz	35.17 Mb	46,XX[20]	nuc ish (GOLIM4/EGFEM1P, MECOM,LRRC34)x2[200],(RUNX1T1,RUNX1)x2[200],(KMT2Ax2)[200],(PML,RARA)x2[200],(MYH11,CBFB)x2[20	

 doi:10.20944/preprints202605.0494.v1

						0],(TP53,NF1)x2[200]	
44	75	CML	CN gain: 1q41q44(222605116_249250621)x2~3CN Loss: 5q15q35.3(93445448_180915260)x1~2CN Gain: (6)x2~3CN Loss: 7q31.2q36.3(114699163_159138663)x2~2CN Gain (8)x2~3CN Gain: 9p24.3q34.12(14326_133694418)x2~3High Copy Gain: 9q34.12q34.3(133696125_141127851)x3~4CN Gain:)13)x2~3CN Gain(21)x2~3CN-LOH: 21q22.12q22.3(36159252_48096251)x2 mos hmzHigh Copy Gain: 22q11.1q11.23(16052962_23593051)x3~4	11.94 Mb	92,XXYY,t(9;22)(q34;q11.2)x2[2]/97,sl,+6,+8,+9,+13,+21[cp3]/47~49,XY,der(9)t(9;22),-22,+idic(22)(q11.2)t(9;22)x2~4[cp2]/94~97,slx2[cp7]/46,XY[6]	nuc ish (ABL1,BCR)x5~6(ABL1 con BCRx4)[71/200]/(ABL1,BCR)x6~8(ABL1 con BCRx5~6)[9/200]	***RUNX1*** p.T128Pfs*17, c.360_381dup *SF3B1* p.K700E, c.2098A>G
45	66	MPN	CN-LOH: 9p24.3p13.3(14326_34106444)x2 hmz	34.1 Mb	46,XX[20]	N/A	***JAK2*** p.V617F, c.1849G>T *SRSF2* p.P95L, c.284C>T *CUX1* p.R147*, c.439C>T
46	36	AML	CN-LOH: 1p36.33p34.3	35.6 Mb	46,XX[20]	nuc ish (GOLIM4/EGFEM1P, MECOM,LRC34)x2[200],(RUNX1T1,RUNX1)x2[200],(KMT2Ax2)[200],(MYH11,CBFB)x2[200],(TP53,NF1)x2[200]	*NPM1* p.W288Cfs*?, c.860_863dup *EZH2* p.Q512Tfs*9, c.1533dup*NRAS* p.G12D, c.35G>A*FBXW7* p.T15_G16insP, c.45_46insCCT *KAT6A* p.R1129*, c.3385C>T
47	45	MDS	CN-LOH: 4q21.1q35.2(78598313_191154276)x2 mos hmz	112.5 Mb	46,XY[20]	N/A	*JAK2* p.V617F, c.1849G>T *NF1* p.S302N, c.905G>A *SF3B1* p.R625G, c.1873C>G ***TET2*** p.Y1345*, c.4035T>A *CUX1* p.P1168Nfs*8, c.3501_3504del

 doi:10.20944/preprints202605.0494.v1

48	74	Post Polycythemia Vera Myelofibrosis	CN-LOH: 9p24.3p22.2(14326_17298289)x2 mos hmzCN-LOH: 9p22.2p21.1(17298329_28218512)x2 mos hmzCN-LOH: 9p21.1p13.3(28223343_35228020)x1 mos hmzCN Loss: 12q24.31(121871114_122658746)x1~2CN Loss: 20q11.22q13.13(34021282_49638524)x1~2	17.3 Mb ; 10.9 Mb ; 7.0 Mb	46,XY[20]	N/A	***JAK2*** p.V617F, c.1849G>T*TET2* p.T1093Kfs*12, c.3278_3281del
49	81	MDS	CN-LOH: 17p12q12(11412940_32496436)x2 hmz CN-LOH: 19q12q13.43(29219850_59128983)x2 mos hmz	21.1 Mb ; 30.0 Mb	46,XX[20]	N/A	Inconclusive
50	70	Myelofibrosis	CN-LOH: 1p36.33p33(49554_47653459)x2 mos hmz CN-LOH: 1p33p21.1(47654724_106645417)x2 mos hmz	47.6 Mb ; 59.0 Mb	46,XX,del(13)(q13q21)[4]/46,XX[16]	nuc ish (D13S319/D13S25x1, D13S1825x2)[42/200]	*ASXL1* p.G646Wfs*12, c.1934dup ***MPL*** p.W515A, c.1543_1544delinsGC
51	78	AML	CN Gain: (13)x2~3CN-LOH: 21q21.1q22.3(23161363_48096251)x2 mos hmz	24.9 Mb	47,XX,+13[19]/46,XX[1]	nuc ish (GOLIM4/EGFEM1P, MECOM,LRRC34)x2[200],(D5S630,EGR1)x2[200],(D7Z1,D7S486)x2[200],(RUNX1T1,RUNX1)x2[200],(KMT2Ax2)[200],(PML,RARA)x2[200],(MYH11,CBFB)x2[200],(TP53,NF1)x2[200]	***RUNX1*** p.A338Rfs*?, c.1011del*SF3B1* p.K700E, c.2098A>G*WRN* p.R369*, c.1105C>T*IKZF1* p.N159S , c.476A>G
52	43	Polycythemia vera (PV)	CN-LOH: 9p24.3p21.1(14326_30182909)x2 mos hmz	30.2 Mb	46,XY[20]	N/A	***JAK2*** p.V617F, c.1849G>T
53	71	AML	CN Gain: 5p15.33p15.1(13301_16565627)x2~3CN Gain: 5p15.1p14.3(16565881_22292443)x2~3CN Gain: 5p14.3q11.2(22294533_51410612)x2~3CN Gain: 5q11.2(51415798_56574452)x1~2CN Loss: 5q23.2q35.3(125084717_180709213)x1~2CN Loss:	11.1 Mb	47~53,XY,dic(5;8)(q11.2;p11.2),add(6)(p22),-7,+add(8)(p11.2),del(12)(p11.2),+r,+2~3mar[cp7]/47~48,sl,+dic(5;8),-add(8)(p11.2)	nuc ish (D5S630x3~4,EGR1x1)[144/200]/(D5S630x6~8,EGR1x2)[26/200],(D7Z1x2,D7S486x1)[155/200]/(D7Z1x4,D7S	***TP53*** p.Y236C, c.707A>G

 doi:10.20944/preprints202605.0494.v1

	6p25.2p25.1(3320346_6035130)x1~2CN Loss: 7p13(43324527_44455565)x1~2CN Loss: 7q11.22q11.23(71049656_72244402)x1~2CN Loss: 7q11.23q21.3(73341591_92861400)x1~2CN Loss: 7q22.1(98418225_101591561)x1~2CN Loss: 7q31.1q36.3(114409885_159122659)x1~2CN Loss: 8p22(16473121_17916887)x1~2CN Gain: 8p22p21.2(18134632_27001659)x2~3CN Gain: 8p12(29918431_32282418)x2~3CN Gain: 8p11.22q22.1(38901877_986591491)x2~3CN Gain: 8q22.1q22.3(98664074_102676394)x2~3CN Gain: 8q22.3q24.23(102678146_138444226)x2~3CN Gain: 8q24.23q24.3(138444604_146364022)x2~3CN Loss: 9q21.2q21.31(79890727_837027782)x1~2CN Loss: 9q21.31q21.32(83792541_86205137)x1~2CN Loss: 12p13.31p11.21(9551628_31241873)x1~2CN-LOH: 17p13.3p12(1389_11100665)x2 hmzCN Loss: 19p13.11p12(19905444_209100795)x1~2CN Loss: 19p12p11(23418781_24594907)x1~2	,-r,+1~3mar[cp7]/90~92,sdlx2[cp2]/46,XY[4]	486x2)[7/200]

A genome-wide map of CN-LOH events from our cohort is shown in Figure 1. A total of 85 CN-LOH calls were detected (median ~2 per case), ranging from focal (<1 Mb) to whole arm (>110 Mb) in size. 42 CN-LOH calls (49% of total) were <25 Mb in length, a common benchmark identified by multiple previous studies, where OGM would likely not detect these calls[14,19,25]. The distribution of CN-LOH calls by chromosome number in our cohort is highlighted in Figure 2A. The most common CN-LOH event detected involved the JAK2 gene on 9p, observed in 37% of all cases evaluated. Frequently, multiple adjacent regions of CN-LOH on 9p are identified, such as in patient 1 (Figure 2B).

 doi:10.20944/preprints202605.0494.v1

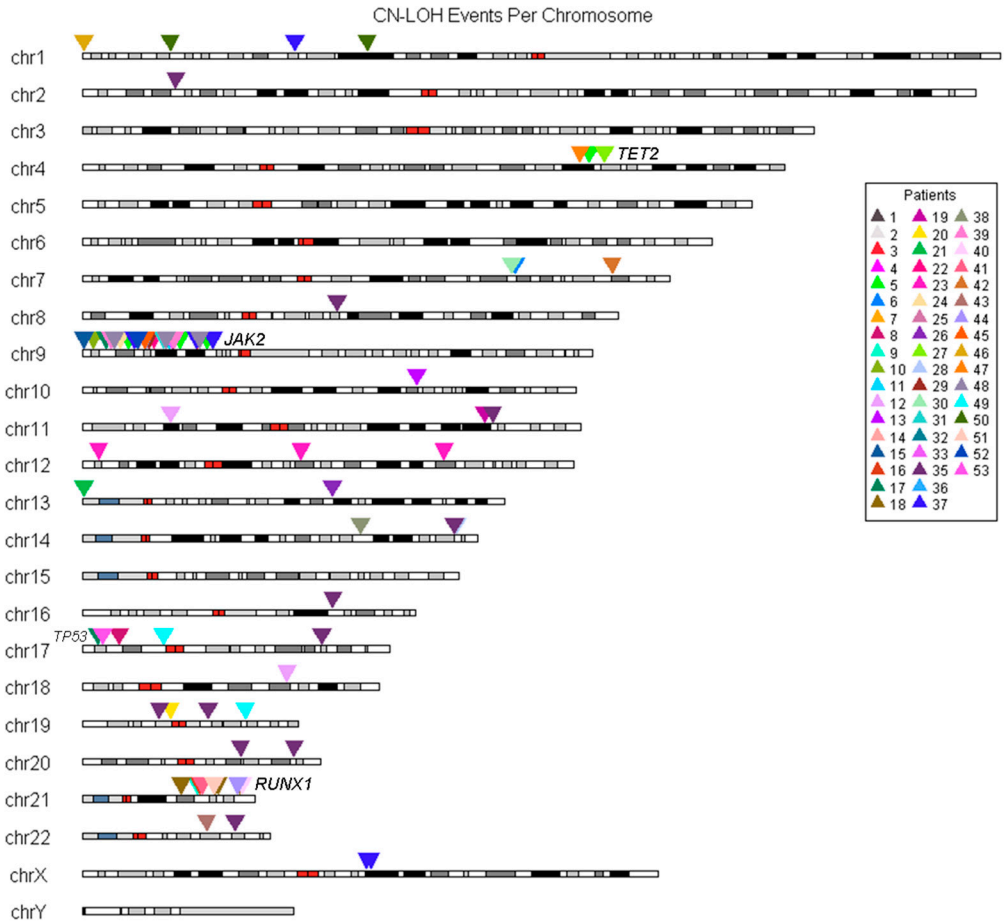

Figure 1. Idiograms of chromosomes 1-22, X, and Y are displayed with CN-LOH events plotted as inverted triangles positioned at approximate genomic locations. Individual cases are distinguished by unique colors. Chromosomes without markers indicate absence of CN-LOH calls in that region. Overlapping CN-LOH events are horizontally offset by 500 kb to improve visibility.

 doi:10.20944/preprints202605.0494.v1

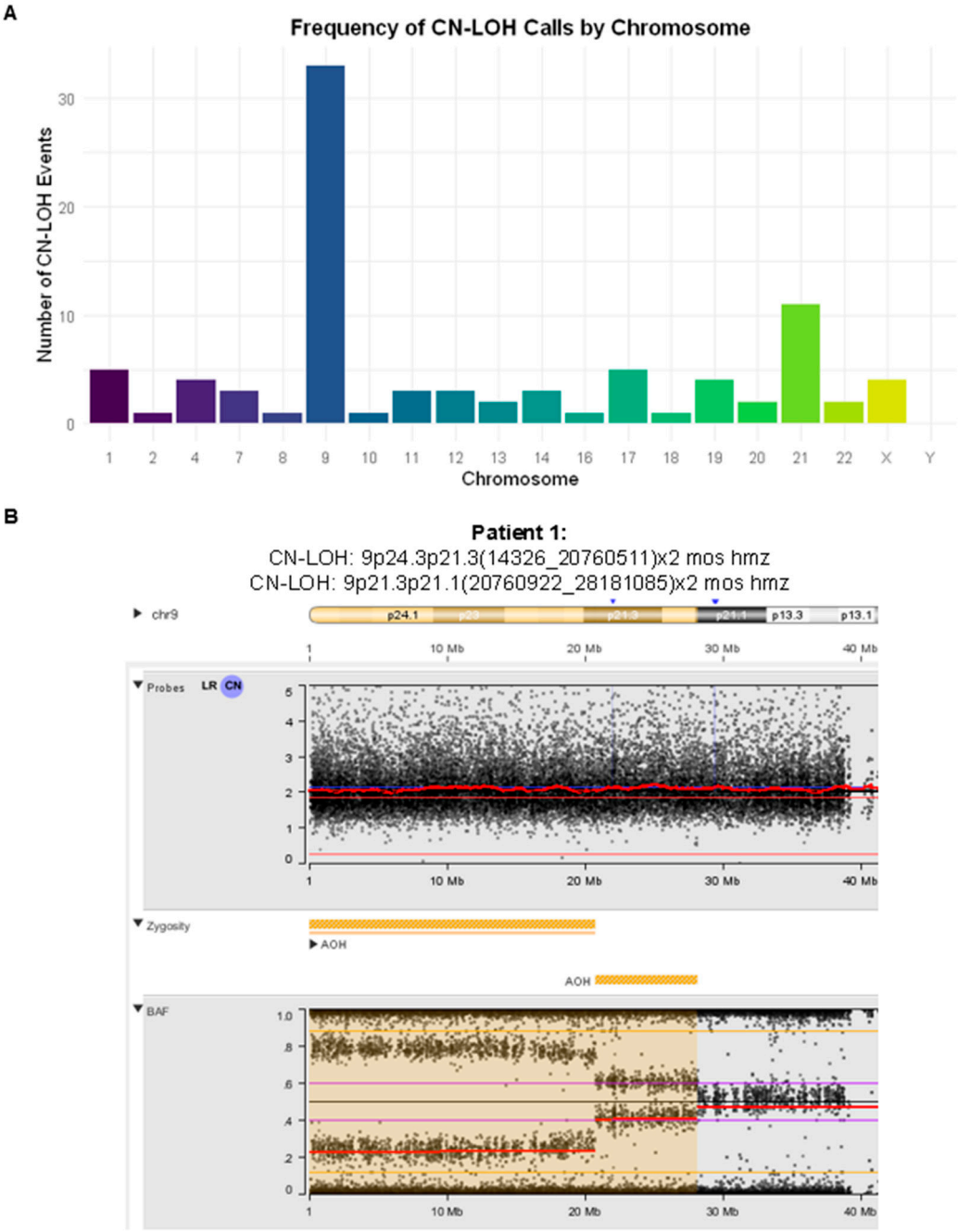

Figure 2. A) Histogram depicting quantity of CN-LOH events by chromosome number (n = 85 events total) **B)** Copy number and B-allele frequency tracks illustrating two adjacent regions of CN-LOH on chromosome 9p (Patient 1). Corresponding ISCN nomenclature reported for the two events is listed above the illustration.

We further investigated the relationship of CN-LOH, karyotype, and FISH results by primary diagnosis, as shown in Table 2. 35 of 53 cases (66%) with CN-LOH detected had a normal karyotype, with the diagnosis of MPN having the highest percentage of cases with normal karyotype occurring in 76%, followed by AML (61%), and MDS (60%). By contrast, six cases showed complex structural abnormalities (≥3 abnormalities) by karyotype. In these cases, OGM would have offered significant advantages for resolving these complex rearrangements while still identifying the large CN-LOH regions. However, CN-LOH events identified by CMA in four of these individuals were <25 Mb in length. For example, in patient 8 (MDS) and patient 53 (AML), a 17p CN-LOH was identified with 20 and 11 Mb in size, respectively, which included the tumor suppressor gene *TP53* (17p13.1) (Figure 3A). *TP53* p.Y234D and p.Y236C NGS variants were also present at 56% and 86% variant allele fraction (VAF), respectively. These findings are consistent with biallelic *TP53* gene inactivation.

 doi:10.20944/preprints202605.0494.v1

Table 2. CN-LOH relationships to karyotype and FISH results by primary diagnosis.

Diagnosis	Total Cases	Karyotype Category		FISH Result			CMA Result	
		<3 abnormalities	≥3 abnormalities	Normal	Positive	Negative	Not Performed	LOH with CN Loss/Gain	LOH without CN Loss/Gain
AML	14 (26%)	3	3	8	3	9	2	6	8
MDS	15 (28%)	5	1	9	1	0	14	8	7
CMML	1 (2%)	0	0	1	1	0	0	0	1
B-cell ALL	1 (2%)	0	1	0	1	0	0	1	0
T-ALL	1 (2%)	0	0	1	1	0	0	1	0
CML	1 (2%)	0	1	0	1	0	0	1	0
Essential Thrombocytopenia (ET)	2 (4%)	0	0	2	0	0	2	0	2
MPN	4 (8%)	1	0	3	0	0	4	0	4
Myelofibrosis (MF)	8 (15%)	2	0	6	1	0	7	2	6
Polycythemia Vera (PV)	6 (11%)	0	1	5	0	0	6	2	4
MPN (CML, ET, MPN, MF, PV)	21 (40%)	3	2	16	2	0	19	5	16

 doi:10.20944/preprints202605.0494.v1

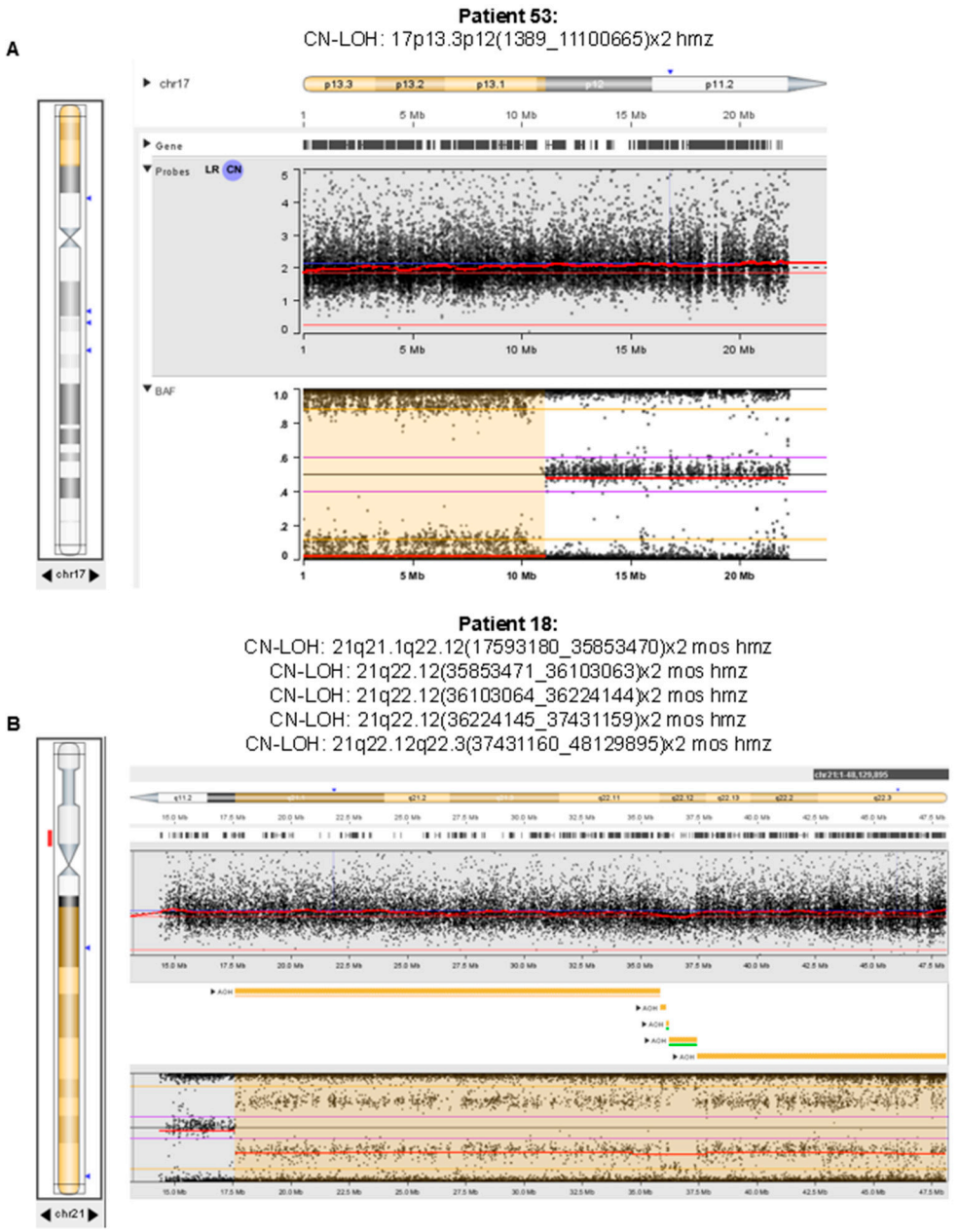

Figure 3. A) Copy number and B-allele frequency tracks illustrating CN-LOH on chromosome 17p involving *TP53* (Patient 53). The corresponding ISCN nomenclature is listed above the illustration. **B)** Copy number and B-allele frequency tracks illustrating four adjacent CN-LOH events on chromosome 21q involving *RUNX1* (Patient 18). The corresponding ISCN nomenclature is listed above the illustration.

Further analysis revealed that 41 of the 53 patients (77.4%) harbored clinically actionable NGS-identified variants within the CN-LOH regions. Genes in these regions included ***FLT3*** (13q12.2) (seen in 2/53 (3.7%) total; 2/14 (14.2%) AML), ***JAK2*** (9p24.1) (20/53 (37.7%) total; 2/14 (14.2%) AML; 1/15 (6.6%) MDS; 16/21 (76.1%) MPN, one case of CMML), ***TET2*** (4q24) (4/53 (7.5%) total; 2/15 (13.3%) MDS; 1/21 (4.7%) MPN; one case of CMML), ***RUNX1*** (21q22.12) (5/53 (9.4%) total; 4/14 (28.6%) AML; one case of CML), ***MPL*** (1p34.2) (2/53 (3.7%) total; 2/21 (9.5%) MPN), ***TP53*** (17p13.1) (2/53 (3.7%) total; one case of MDS, one case of AML), ***EZH2*** (7q36.1) (seen in 2/53 (3.7%) total; 2/15 (13.3%) MDS), ***NOTCH1*** (9q34.3) (patient 15 with T-ALL), ***CDKN2A*** (9p21.3) (patient 31 with B-ALL), ***BCOR*** (Xp11.4) (patient 34 with MDS), ***SETBP1*** (18q12.3) (patient 12 with MDS/MPN), ***U2AF1*** (21q22.3) (patient 40 with MDS). Although *TET2* single- and double-hit mutations were detected in 4/14 (28.6%) AML cases by NGS, CN-LOH was not present. CN-LOH of 21q involving *RUNX1* mutation, the sole abnormality detected in AML cases, was associated with a normal or intermediate-risk

 doi:10.20944/preprints202605.0494.v1

karyotype; an example is shown for patient 18 (Figure 3B). These findings highlight the complementary value of integrating CMA with NGS, as CN-LOH can augment the impact of existing variants.

3.2. Newly Diagnosed B-ALL cases

To better understand OGM's advantages with respect to our own testing cohort, we identified 14 patients with newly diagnosed B-ALL who had concurrent karyotyping, FISH, and CMA performed among our total CMA testing cohort of 327 patients. All newly diagnosed B-ALL patients at our institution undergo CMA. The full clinical results of our B-ALL cohort are summarized in Tables 1 and 3. The average patient age was 53 years, with 11 male and 3 female cases.

Table 3. Newly diagnosed B-ALL cohort demographic, cytogenetic, and molecular characteristics.

Patient	Age	Diagnosis	CMA Events	Size of LOH:	Karyotype	FISH	NGS
1	72	F	B-cell ALL	CN Loss: 6q23.3(135360827_135437106)x1~2 CN Gain: 9q34.12q34.3(133736858_141127851)x2~3 CN Gain: 10p15.3p11.1(60523_39154220)x2~3 CN Gain: 10q11.21q26.3(42355302_135499683)x2~3 CN Gain: 22q11.1q11.23(16052962_23629737)x2~3	0.08 Mb 7.4 Mb 39.1 Mb 93.1 Mb 7.6 Mb	46,XX,t(9;22)(q34;q11.2)[15]/47,sdl,+der(22)t(9;22)[2]/48,sdl,+10[3]	**Bone Marrow:** nuc ish (ABL1,BCR)x3(ABL1 con BCRx2)[166/200]/(ABL1,BCR)x4(ABL1 con BCRx3)[4/200],(IKZF1,7q11.21)x2[200]
2	57	F	B-cell ALL	CN Loss: (7)x1~2	159.1 Mb	45,XX,-7,t(9;22)(q34;q11.2)[12]/46,XX[8]	**Peripheral Blood:** nuc ish (ABL1,BCR)x3(ABL1 con BCRx2)[83/200],(IKZF1,7q11.21)x1[80/200],(CDKN2A,CEP9)x2[200]
3	49	M	B-cell ALL	CN Loss: 7p12.2(50417522_50462935)x1~2	0.05 Mb	46,XY,t(9;22)(q34;q11.2)[20]	**Peripheral Blood:** nuc ish(ABL1,BCR)x3(ABL1 con BCRx2)[175/200],(IKZF1,7q11.21)x2[200]
4	60	M	B-cell ALL	CN Loss: 7p22.3p14.1(16487_37534044)x1~2 CN Loss: 7p14.1p12.1(39905801_53103888)x1~2 CN Gain: (8)x2~3 CN Loss: 9p24.3p21.3(14326_21753137)x1~2 Homozygous Copy Loss: 9p21.3(21753138_21984661)x0~1 CN Loss: 9p21.3(21984662_38792812)x1~2	37.5 Mb 13.2 Mb 146.4 Mb 21.7 Mb 0.2 Mb 16.8 Mb 1.9 Mb 2.6 Mb 0.08 Mb 0.3 Mb 26.2 Mb	45,XY,-7,der(9)t(7;9)(q11.2;p10),(IKZF1x1,7q3)[15]/46,XY[5]	**Peripheral Blood:** nuc ish (CDKN2Ax1,CEP9x2)[24/200],(IKZF1x1,7q11.21x2)[22/200],(ABL1,BCR)x2[200] **Bone Marrow:**

 doi:10.20944/preprints202605.0494.v1

				CN Loss: 15q13.2q13.3(30915983_32795582)x1 CN Loss: Xp22.33(60425_2698170)x1~2 High Copy Gain: Xq25(123154718_123237996)x3 CN Loss: Xq28(154936819_155236204)x1~2 Hemizygous Copy Loss: Yp11.31q12(2654333_28817636)x0~1			nuc ish (ABL2x2)[200],(PDGFRBx2)[200],(MYCx2)[200],(JAK2x2)[200],(EPORx2)[200]
5	70	M	B-cell ALL	arr (X,Y)x1,(1-22)x2	N/A	46,XY,t(9;22)(q34;q11.2)[3]/46,XY[17]	**Peripheral Blood:** nuc ish (ABL1,BCR)x3(ABL1 conBCRx2)[115/200],(IKZF1,7q11.21)x2[200] **Bone Marrow:** nuc ish (ABL1,BCR)x3(ABL1 conBCRx2)[115/200],(IKZF1,7q11.21)[200],(CDKN2A,CEP9)x2[200]
6	63	M	B-cell ALL	Cancelled because low-hypodiploid karyotype was detected.	N/A	34~36,XY,-2,-3,-7,-9,-12,-13,-15,-16,-17,-20,-22[cp11]/46,XY[9]	**Peripheral Blood:** nuc ish (CDKN2A,CEP9)x1[118/200],(IKZF1,7q11.21)x1[108/200],(ABL1x1,BCRx2)[78/200]/(ABL1,BCR)x1[42/200/(ABL1x2,BCRx3)[16/200]/(ABL1x1,BCRx3)[5/200],(ETV6x1,RUNX1x2)[112/200],(KMT2Ax2)[200] **Bone Marrow:** nuc ish (ABL1x2,BCRx1)[135/200],(IKZF1,7q11.21)x2[200],(CDKN2A,CEP9)[200],(KMT2Ax2)[200],(ETV6,RUNX1)x2[200]
7	37	M	B-cell ALL	arr (X,Y)x1,(1-22)x2 (Low-level copy number alterations of 1-4, 6, 17, and 22 below reporting threshold)	N/A	46,XY[20]	
8	24	M	B-cell ALL	CN Gain: (5)x2~3 CN Gain: (8)x2~3 CN Gain: (10)x2~3 CN Gain: (21)x2~3	180.9 Mb 146.4 Mb 135.5 Mb 48.1 Mb	51,XY,+X,+5,+8,+10,-16,+der(19)t(1;19)(q23;p13.3),+21[	**Bone Marrow:** nuc ish (CRLF2x2)(3'CRLF2 sep 5'CRLF2x1)[5/

 doi:10.20944/preprints202605.0494.v1

						2]/46,XY[18]	200]/(CRLF2x3)(3'CRLF2 sep 5'CRLF2x1)[9/200],(ABL2x3)[19/200],(MYCx3)[19/200],(ETV6x2,RUNX1x3)[19/200],(P2RY8x3)[18/200],(PDGFRBx3)[16/200],(KMT2Ax3)[9/200],(IKZF1,7q11,21)x2[200],(ABL1,BCR)x2[200],(CDKN2A,CEP9)x2[200],(JAK2x2)[200],(EPORx2)[200]
9	54	M	B-cell ALL	CN Loss: 9p21.3p13.1(20621028_39097054)x1~2	18.5 Mb	46,XY,del(9)(p23p21)[10]/46,XY[10]	**Bone Marrow:** nuc ish (CDKN2Ax1, CEP9x2)[129/200],(EPORx2)(3'EPOR sep 5'EPORx1)[5/200],(ABL2x2)[200],(PDGFRBx2)[200],(IKZF1,7q11.21)x2[200],(MYCx2)[200],(ABL1,BCR)x2[200],(JAK2x2)[200],(KMT2Ax2)[200]
10	79	M	B-cell ALL	arr (X,Y)x1,(1-22)x2	N/A	46,XY,t(8;22)(p11.2;q11.2)[5]/46,XY[15]	**Bone Marrow:** nuc ish (FGFR1,D8Z2)x2(5'FGFR1 sep 3'FGFR1x1)[310/500],(ABL1x2,BCRx3)[92/200],(MYCx2)[200],(IGH,BCL2)x2[500]
11	50	M	B-cell ALL	CN Loss: 3p21.31(47129903_47204518)x1~2 CN Loss: 3q13.2(112053956_112219535)x1~2 CN Loss: 7p12.2(50411178_50463667)x1 CN Loss: 9p21.3(19926411_21833882)x1~2 Homozygous Copy Loss: 9p21.3(21833883_2207358)x0~1 CN Loss: 9p21.3(22007359_22706144)x1~2 CN Loss:	0.07 Mb 0.17 Mb 0.05 Mb 1.9 Mb 0.17 Mb 0.7 Mb 0.31 Mb 0.09 Mb	46,XY,der(3)add(3)(p25)add(3)(q27)[13]/46,XY[7]	**Peripheral Blood:** nuc ish ((CRLF2x2)(3'CRLF2 sep 5'CRLF2x1)[85/200],(ABL1,BCR)x2[200],(P2RY8x2)[200] **Bone Marrow:**

 doi:10.20944/preprints202605.0494.v1

				12q21.33(92227078_92537956)x1~2 Homozygous Copy Loss: 13q14.2(48985639_49073897)x0~1)			nuc ish (BCL6x2)[200]
12	74	F	B-cell ALL	CN Loss: (7)x1~2	159.1 Mb	45,XX,-7,t(9;22)(q34;q11.2)[3]/46,XX[17]	**Peripheral Blood:** nuc ish (ABL1,BCR)x3 (ABL1 con BCRx2)[78/200],(IKZF1,7q11.21)x1[34/200],(CDKN2A,CEP9)x2[200],(KMT2Ax2)[200],(ETV6,RUNX1)x2[200] **Bone Marrow:** nuc ish (ABL1x2,BCRx3)[8/200],(SCFD2,LNX,PDGFRA/KIT)x2[200],(IKZF1,7q11.21)x2[200],(FGFR1,D8Z2)x2[200],(MYCx2)[200],(CDKN2A,CEP9)x2[200],(JAK2x2)[200],(KMT2Ax2)[200],(ETV6,RUNX1)x2[200],(FLT3x2)[200],(EPORx2)[200]
13	24	M	B-cell ALL	CN Gain: 1q12q44(142544928_249212725)x2~3 CN Gain: (10)x2~3 CN Gain: (21)x2~3 CN Gain (22)x2~3	106.7 Mb 135.5 Mb 48.1 Mb 51.3 Mb	49,XY,+1,+22,inc[1]/46,XY[19]	**Bone Marrow:** nuc ish (ABL1x2,BCRx3)[8/200],(SCFD2,LNX,PDGFRA/KIT)x2[200],(IKZF1,7q11.21)x2[200],(FGFR1,D8Z2)x2[200],(MYCx2)[200],(CDKN2A,CEP9)x2[200],(JAK2x2)[200],(KMT2Ax2)[200],(ETV6,RUNX1)x2[200],(FLT3x2)[200],(EPORx2)[200]
14	24	M	B-cell ALL	CN Gain: 1q12q44(142544928_249212725)x2~3 CN Gain: (10)x2~3 CN Gain: (21)x2~3 CN Gain (22)x2~3	106.7 Mb 135.5 Mb 48.1 Mb 51.3 Mb	49,XY,+1,+22,inc[1]/46,XY[19]	**Bone Marrow:** nuc ish (ABL1x2,BCRx3)[8/200],(SCFD2,LNX,PDGFRA/KIT)x2[200],(IKZF1,7q11.21)x2[200],(FGFR1,D8Z2)x2[200],(MYCx2)[200],(CDKN2A,CEP9)x2[200],(JAK2x2)[200],(KMT2Ax2)[200],(ETV6,RUNX1)x2[200],(FLT3x2)[200],(EPORx2)[200]

Most of our B-ALL cohort demonstrated both abnormal karyotype and FISH results. Our laboratory routinely performs *BCR::ABL1* "STAT" FISH testing on peripheral blood, followed by a cascade of additional probes, including *KMT2A, IKZF1, CDKN2A, ETV6::RUNX1,* and *IGH*. Cases

 doi:10.20944/preprints202605.0494.v1

reported positive for BCR::ABL1 reflex to a Ph-like panel, including *ABL2, PDGFRB, JAK2, EPOR*, and *MYC* FISH probes. Further, *CRLF2*-positive immunophenotypes identified by flow cytometry trigger *CRLF2* and *P2RY8* FISH confirmatory testing. Collectively, this workflow often results in numerous FISH probes per case, even when many assays yield normal results. For example, patient 13 required 11 separate FISH assays, 10 of which were normal, as shown in **Table 3**.

CN-LOH was only identified in one patient (patient 31, Table 1) and was >25 Mb in length. However, focal copy-number changes <25 Mb were identified in 7 of the 13 successful CMA studies. Of note, one patient had cancelled CMA because a low-hypodiploid karyotype was detected, with high prognostic risk.

 doi:10.20944/preprints202605.0494.v1

4. Discussion

Our retrospective study highlights CN-LOH as a frequent and clinically significant finding in neoplastic testing. In our cohort, nearly half of the CN-LOH events observed were <25 Mb in size and below the conventional OGM reporting threshold. Despite their smaller sizes, they encompass mutations in critical driver genes with direct implications for risk stratification and treatment selection, particularly when accompanied by NGS variants within the CN-LOH region. CMA offers distinct advantages derived from its single-nucleotide polymorphism (SNP)- based array design. The platform provides genome-wide coverage, enabling the detection of submicroscopic CN changes and copy-neutral events such as CN-LOH, uniparental disomy (UPD) and regions of homozygosity[6]. For example, CN-LOH involving the *TP53* gene, along with a clinically actionable *TP53* variant identified by NGS, has significant prognostic value in MDS and AML patients. The resulting biallelic inactivation of *TP53* in MDS (patient 8) meets the criteria for the MDS-defining genetic subtype, MDS with biallelic *TP53* inactivation (MDS-bi*TP53*), per the World Health Organization (WHO) and National Comprehensive Cancer Network (NCCN.org), and is associated with increased bone marrow blasts and a high risk of progression to leukemia and death, independent of treatment[26,27]. In AML with biallelic *TP53* mutations (patient 53), individuals fall into a high-risk subset within the poor prognostic category of recurrent genetic abnormalities. Accurate determination of *TP53* biallelic status is increasingly critical for guiding precision medicine decisions, including recommendations for hematopoietic cell transplantation or clinical trial enrollment[28]. Detecting focal CN-LOH events involving the *TP53* locus provides essential insight into biallelic involvement, information that would be missed by OGM alone.

In our study, several 9p CN-LOH events co-occurred with *JAK2* mutations identified by NGS, a pattern associated with increased mutation burden, clonal expansion, and a higher risk of progression to myelofibrosis or accelerated phase, underscoring the importance of detecting these copy-neutral events[29,30]. Two AML patients harbored FLT3 internal tandem duplications with CN-LOH spanning the *FLT3* locus; prior work has linked this combination to higher relapse rates and poorer overall survival[31]. Additionally, *MPL* W515 mutations accompanied by CN-LOH involving the *MPL* locus were observed in patients with myelofibrosis. Acquired 1p CN-LOH affecting *MPL* has been implicated in fibrotic transformation in MPNs carrying *MPL* mutations[32].

CN-LOH involving 4q, encompassing *TET2*, was also frequently observed. *TET2* mutations are common in MDS, AML, and clonal hematopoiesis, and are associated with worse prognosis in MDS[33]. *TET2* inactivation through CN-LOH has been linked to increased proliferation, inflammation, and self-renewal[34]. Although not a distinct disease subtype, patients with high-VAF *TET2* mutations and CN-LOH carry a high risk of progressing from early leukemic states, such as clonal hematopoiesis, to overt malignancy. Early identification of these high-risk *TET2* events may enable earlier intervention and risk-reduction strategies. CN-LOH of 21q is another recurrent abnormality in AML[31,35]. In our cohort, 21q CN-LOH co-occurring with a pathogenic *RUNX1* variant was detected in 28% of AML cases. While one prior study reported favorable outcomes in AML with 21q CN-LOH, *RUNX1* mutation status was not evaluated[36]. In contrast, biallelic *RUNX1* alteration resulting from CN-LOH combined with a *RUNX1* sequence variant has been associated with a worse prognosis compared with monoallelic mutation[31,37]. These findings underscore the importance of integrating CMA and NGS for accurate clinical interpretation and highlight CMA's high-resolution CN-LOH detection in guiding clinical decision-making.

OGM provides superior structural variant detection, high-resolution breakpoint mapping, and the ability to consolidate multiple cytogenetic workflows into a single assay[12,14,18]. These advantages are especially valuable in cases with complex rearrangements that are difficult to resolve by conventional karyotyping. However, practical considerations, including institutional resources and technical requirements, must be addressed when developing an OGM-based workflow. Implementation requires a significant upfront investment, including ultra-high molecular weight DNA extraction, specialized instrumentation, and substantial computational infrastructure, which may be challenging for smaller laboratories with limited budgets or support. Although these

 doi:10.20944/preprints202605.0494.v1

barriers are expected to diminish as the technology matures, they currently remain a constraint for many centers.

Across myeloid malignancies, including MPN, MDS, and AML, 60–76% of cases showed normal karyotypes with CN-LOH identified only by CMA (Table 2). Recent data indicate limited clinical utility of OGM in MPN: aside from detecting KMT2A-PTD in a subset of karyotypically normal cases, OGM did not reveal additional tier 1 or tier 2 copy-number or structural variants in MDS or MDS/MPN, nor did it identify any new tier 1 abnormalities in myeloid malignancies with complex karyotypes. In AML, tier 2 OGM-detected abnormalities mainly involved *MECOM*, *KMT2A*, and *NUP98* rearrangements,[38] most of which would be captured by CMA and the AML FISH panel used in this study for adult and elderly patients; *NUP98* FISH may be useful in pediatric settings. Based on these findings, we propose that laboratories without OGM perform karyotyping, a heme NGS panel, and CMA for MPN, MDS, and MDS/MPN, with reflex FISH testing based on karyotype findings for future minimal residual disease detection. For adult AML, we suggest karyotyping, targeted FISH for actionable rearrangements requiring rapid turnaround, CMA, and a heme NGS panel. For laboratories implementing OGM, testing should include limited FISH for urgent actionable rearrangements, CMA until segmental or focal CN-LOH detection is available in OGM, a heme NGS panel, and OGM.

Newly diagnosed B-ALL requires extensive cytogenetic evaluation, often using multiple targeted FISH probes that are costly, labor-intensive, and restricted to predefined loci. OGM offers a comprehensive, streamlined alternative. Although it cannot detect focal CN-LOH, these events are less common in B-ALL than in myeloid neoplasms[39]. In contrast, the structural variants, aneuploidies, fusions, and rearrangements that characterize B-ALL are strengths of OGM detection. In our cohort, OGM would have identified all clinically relevant abnormalities targeted by FISH in a single assay, reducing cost, labor, and turnaround time. Many focal copy-number alterations detected by CMA, such as *CDKN2A*, *RB1*, and *IKZF1* losses, also fall within OGM's resolution for copy-number gains and losses (~500 bp), and OGM would concurrently detect structural rearrangements missed by CMA. We propose that diagnostic workflows for B- and T-ALL include karyotype, FISH, a heme NGS panel, and CMA for laboratories without OGM. For laboratories with OGM, we propose limiting FISH to rapidly actionable rearrangements while incorporating OGM and a heme NGS panel.

Although whole-genome sequencing (WGS) provides the most comprehensive assay for detecting CN changes, SVs, and CN-LOH, its clinical adoption is limited by the substantial sequencing depth, computational resources, and bioinformatics expertise required. Similar challenges apply to combined NGS-plus-SNP approaches and whole-exome sequencing (WES)[40]. WES can infer CN-LOH using BAF and read-depth modeling, but sensitivity is far lower than with WGS or SNP arrays due to limited exonic coverage. Accordingly, WGS, WES, and hybrid NGS-plus-SNP workflows were not included in the proposed testing recommendations for routine clinical use.

The limitations of this study include its retrospective design and modest cohort size, which constrain generalizability. Because OGM was not directly performed, concordance could not be empirically evaluated; incorporating OGM in future analyses would strengthen the findings. However, prior reports indicating limited OGM sensitivity for focal CN-LOH suggest that many such events in our cohort would likely remain undetected[41]. Larger, multi-institutional studies across diverse hematologic malignancies, integrating karyotyping, FISH, CMA, OGM, and NGS, are needed to better define the complementary roles of these technologies and guide test selection based on available resources.

5. Conclusions

While OGM represents a significant advance in cytogenetic technology, our analysis demonstrates that CMA remains an essential diagnostic resource for detecting clinically relevant CN LOH events. Rather than replacement, we suggest that the future of cytogenetic testing lies in

 doi:10.20944/preprints202605.0494.v1

strategic integration, where the strengths of multiple technologies are utilized to deliver a complete and actionable genetic profile. This combined approach ensures that no significant event is overlooked in the pursuit of precision oncology.

Author Contributions: Conceptualization, A.M. and S.G.; methodology, A.M., P.G., and S.G.; software, A.M.; validation, A.M., P.G., and S.G.; formal analysis, A.M., P.G., and S.G.; investigation, A.M., P.G., and S.G.; resources, A.M.; data curation, A.M.; writing—original draft preparation, A.M.; writing—review and editing, P.G. and S.G.; visualization, S.G.; supervision, S.G.; project administration, S.G.; funding acquisition, S.G. All authors have read and agreed to the published version of the manuscript.

Funding: This research received no external funding.

Institutional Review Board Statement: The study was conducted in accordance with the Declaration of Helsinki and approved by the Institutional Review Board at The University of Kansas Medical Center (Study ID: STUDY00160636, approved on 20th June 2024).

Informed Consent Statement: Patient consent was waived due to all testing being performed as a part of routine clinical care. The retrospective review was approved by an institutional review board (Study ID: STUDY00160636, approved on 20th June 2024).

Data Availability Statement: The data that support the findings of this study are available on request from the corresponding author. The data are not publicly available due to privacy or ethical restrictions.

Acknowledgments: We thank the entire staff of the Cytogenetics Laboratory and Microarray lead technologist Traci Troyer at The University of Kansas Health System for their assistance with this work.
Conflicts of Interest: The authors declare no conflicts of interest.

Abbreviations

The following abbreviations are used in this manuscript:

AML	Acute myeloid leukemia
ALL	Acute lymphoblastic leukemia
B-ALL	B-cell acute lymphoblastic leukemia
CMA	Chromosomal microarray
CN	Copy number
CN-LOH	Copy-neutral loss of heterozygosity
CMML	Chronic myelomonocytic leukemia
FISH	Fluorescence in situ hybridization
MDS	Myelodysplastic syndrome
MPN	Myeloproliferative neoplasm
NGS	Next-generation sequencing
NCCN	National Comprehensive Cancer Network
OGM	Optical genome mapping
UPD	Uniparental disomy
VAF	Variant allele fraction
WHO	World Health Organization

References

1. S. L. Gersen and M. B. Keagle, “The Principles of Clinical Cytogenetics.”
2. P. R. Gonzales, “Integration of Newer Genomic Technologies into Clinical Cytogenetics Laboratories,” *Genes (Basel).*, vol. 16, no. 6, Jun. 2025, doi: 10.3390/GENES16060688.
3. P. R. Gonzales, A. J. Carroll, and B. R. Korf, “Overview of clinical cytogenetics,” *Curr. Protoc. Hum. Genet.*, vol. 2016, pp. 8.1.1-8.1.13, 2016, doi: 10.1002/0471142905.hg0801s89.
4. L. TJ *et al.*, “Genomic and epigenomic landscapes of adult de novo acute myeloid leukemia,” *N. Engl. J. Med.*, vol. 368, no. 22, pp. 2059–2074, May 2013, doi: 10.1056/NEJMOA1301689.

 doi:10.20944/preprints202605.0494.v1

5. F. M. Mikhail *et al.*, "Technical laboratory standards for interpretation and reporting of acquired copy-number abnormalities and copy-neutral loss of heterozygosity in neoplastic disorders: a joint consensus recommendation from the American College of Medical Genetics and Geno…," *Genetics in Medicine*, vol. 21, no. 9, pp. 1903–1915, Sep. 2019, doi: 10.1038/s41436-019-0545-7.
6. D. T. Miller *et al.*, "Consensus Statement: Chromosomal Microarray Is a First-Tier Clinical Diagnostic Test for Individuals with Developmental Disabilities or Congenital Anomalies," *Am. J. Hum. Genet.*, vol. 86, no. 5, pp. 749–764, May 2010, doi: 10.1016/j.ajhg.2010.04.006.
7. S. M. Jalal and M. E. Law, "Utility of multicolor fluorescent in situ hybridization in clinical cytogenetics," *Genetics in Medicine*, vol. 1, no. 5, pp. 181–186, 1999, doi: 10.1097/00125817-199907000-00003.
8. J. T. Mascarello *et al.*, "Section E9 of the American College of Medical Genetics technical standards and guidelines: Fluorescence in situ hybridization," *Genetics in Medicine*, vol. 13, no. 7, pp. 667–675, 2011, doi: 10.1097/GIM.0b013e3182227295.
9. C. D. Bangs and T. A. Donlon, "Metaphase chromosome preparation from cultured peripheral blood cells," *Curr. Protoc. Hum. Genet.*, vol. Chapter 4, 2005, doi: 10.1002/0471142905.HG0401S45.
10. A. Ronaghy, R. K. Yang, J. D. Khoury, and R. Kanagal-Shamanna, "Clinical Applications of Chromosomal Microarray Testing in Myeloid Malignancies," *Curr. Hematol. Malig. Rep.*, vol. 15, no. 3, pp. 194–202, Jun. 2020, doi: 10.1007/S11899-020-00578-1.
11. P. Dremsek, T. Schwarz, B. Weil, A. Malashka, F. Laccone, and J. Neesen, "Optical Genome Mapping in Routine Human Genetic Diagnostics-Its Advantages and Limitations," *Genes (Basel).*, vol. 12, no. 12, Dec. 2021, doi: 10.3390/GENES12121958.
12. N. S. Sahajpal, H. Barseghyan, R. Kolhe, A. Hastie, and A. Chaubey, "Optical Genome Mapping as a Next-Generation Cytogenomic Tool for Detection of Structural and Copy Number Variations for Prenatal Genomic Analyses," *Genes (Basel).*, vol. 12, no. 3, Mar. 2021, doi: 10.3390/GENES12030398.
13. H. Barseghyan *et al.*, "Optical Genome Mapping as a Potential Routine Clinical Diagnostic Method," *Genes (Basel).*, vol. 15, no. 3, Mar. 2024, doi: 10.3390/GENES15030342.
14. R. Kanagal-Shamanna *et al.*, "Integration of Optical Genome Mapping in the Cytogenomic and Molecular Work-Up of Hematological Malignancies: Expert Recommendations From the International Consortium for Optical Genome Mapping," *Am. J. Hematol.*, vol. 100, no. 6, pp. 1029–1048, Jun. 2025, doi: 10.1002/AJH.27688.
15. K. Neveling *et al.*, "Next-generation cytogenetics: Comprehensive assessment of 52 hematological malignancy genomes by optical genome mapping," *Am. J. Hum. Genet.*, vol. 108, no. 8, pp. 1423–1435, Aug. 2021, doi: 10.1016/j.ajhg.2021.06.001.
16. A. C. Smith, K. Neveling, and R. Kanagal-Shamanna, "Optical genome mapping for structural variation analysis in hematologic malignancies," *Am. J. Hematol.*, vol. 97, no. 7, pp. 975–982, Jul. 2022, doi: 10.1002/AJH.26587.
17. H. Yang *et al.*, "High-resolution structural variant profiling of myelodysplastic syndromes by optical genome mapping uncovers cryptic aberrations of prognostic and therapeutic significance," *Leukemia*, vol. 36, no. 9, pp. 2306–2316, Sep. 2022, doi: 10.1038/S41375-022-01652-8.
18. I. Schrauwen *et al.*, "Optical genome mapping unveils hidden structural variants in neurodevelopmental disorders," *Sci. Rep.*, vol. 14, no. 1, Dec. 2024, doi: 10.1038/S41598-024-62009-Y.
19. B. Levy *et al.*, "Multisite Evaluation and Validation of Optical Genome Mapping for Prenatal Genetic Testing," *Journal of Molecular Diagnostics*, vol. 26, no. 10, pp. 906–916, Oct. 2024, doi: 10.1016/j.jmoldx.2024.06.006.
20. A. L. Godfrey *et al.*, "JAK2V617F homozygosity arises commonly and recurrently in PV and ET, but PV is characterized by expansion of a dominant homozygous subclone," *Blood*, vol. 120, no. 13, p. 2704, Sep. 2012, doi: 10.1182/BLOOD-2012-05-431791.
21. H. Makishima *et al.*, "CBL, CBLB, TET2, ASXL1, and IDH1/2 mutations and additional chromosomal aberrations constitute molecular events in chronic myelogenous leukemia," *Blood*, vol. 117, no. 21, p. e198, May 2011, doi: 10.1182/BLOOD-2010-06-292433.
22. F. Delhommeau *et al.*, "Mutation in TET2 in myeloid cancers," *N Engl J Med*, vol. 360, no. 22, pp. 2289–2301, 2009, doi: 10.1056/NEJMoa0810069.

 doi:10.20944/preprints202605.0494.v1

23. M. Olivier, M. Hollstein, and P. Hainaut, "TP53 Mutations in Human Cancers: Origins, Consequences, and Clinical Use," *Cold Spring Harb. Perspect. Biol.*, vol. 2, no. 1, p. a001008, 2010, doi: 10.1101/CSHPERSPECT.A001008.
24. M. M. Li *et al.*, "Standards and Guidelines for the Interpretation and Reporting of Sequence Variants in Cancer: A Joint Consensus Recommendation of the Association for Molecular Pathology, American Society of Clinical Oncology, and College of American Pathologists," *Journal of Molecular Diagnostics*, vol. 19, no. 1, pp. 4–23, Jan. 2017, doi: 10.1016/j.jmoldx.2016.10.002.
25. H. Barseghyan, A. W. C. Pang, B. Clifford, M. A. Serrano, A. Chaubey, and A. R. Hastie, "Comparative Benchmarking of Optical Genome Mapping and Chromosomal Microarray Reveals High Technological Concordance in CNV Identification and Additional Structural Variant Refinement," *Genes (Basel).*, vol. 14, no. 10, p. 1868, Oct. 2023, doi: 10.3390/GENES14101868/S1.
26. Y. Abaza *et al.*, "NCCN Guidelines Version 1.2026 Myelodysplastic Syndromes Krist Biakanja III Patient Advocate," 2025, Accessed: Dec. 04, 2025. [Online]. Available: https://www.nccn.org/home/member-
27. J. D. Khoury *et al.*, "The 5th edition of the World Health Organization Classification of Haematolymphoid Tumours: Myeloid and Histiocytic/Dendritic Neoplasms," *Leukemia*, vol. 36, no. 7, pp. 1703–1719, Jul. 2022, doi: 10.1038/S41375-022-01613-1.
28. S. Urrutia, T. N. Wong, and D. C. Link, "A clinical guide to TP53 mutations in myeloid neoplasms," *Blood*, vol. 146, no. 18, pp. 2157–2167, Oct. 2025, doi: 10.1182/BLOOD.2025029691.
29. E. Rumi *et al.*, "Identification of genomic aberrations associated with disease transformation by means of high-resolution SNP array analysis in patients with myeloproliferative neoplasm," *Am. J. Hematol.*, vol. 86, no. 12, pp. 974–979, Dec. 2011, doi: 10.1002/AJH.22166.
30. T. Klampfl *et al.*, "Genome integrity of myeloproliferative neoplasms in chronic phase and during disease progression," *Blood*, vol. 118, no. 1, pp. 167–176, Jul. 2011, doi: 10.1182/BLOOD-2011-01-331678.
31. X. Xu *et al.*, "Assessing copy number abnormalities and copy-neutral loss-of-heterozygosity across the genome as best practice in diagnostic evaluation of acute myeloid leukemia: An evidence-based review from the cancer genomics consortium (CGC) myeloid neoplasms workin…," *Cancer Genet.*, vol. 228–229, pp. 218–235, Dec. 2018, doi: 10.1016/j.cancergen.2018.07.005.
32. E. Rumi *et al.*, "Acquired copy-neutral loss of heterozygosity of chromosome 1p as a molecular event associated with marrow fibrosis in MPL-mutated myeloproliferative neoplasms," *Blood*, vol. 121, no. 21, pp. 4388–4395, May 2013, doi: 10.1182/BLOOD-2013-02-486050.
33. C. C. S. Yeung *et al.*, "Impact of copy neutral loss of heterozygosity and total genome aberrations on survival in myelodysplastic syndrome," *Modern Pathology*, vol. 31, no. 4, pp. 569–580, Apr. 2018, doi: 10.1038/modpathol.2017.157.
34. K. Moran-Crusio *et al.*, "Tet2 Loss Leads to Increased Hematopoietic Stem Cell Self-Renewal and Myeloid Transformation," *Cancer Cell*, vol. 20, no. 1, pp. 11–24, 2011, doi: 10.1016/J.CCR.2011.06.001.
35. F. P. G. Silva *et al.*, "Genome wide molecular analysis of minimally differentiated acute myeloid leukemia," *Haematologica*, vol. 94, no. 11, pp. 1546–1554, Nov. 2009, doi: 10.3324/HAEMATOL.2009.009324.
36. C. M. Gronseth *et al.*, "Prognostic significance of acquired copy-neutral loss of heterozygosity in acute myeloid leukemia," *Cancer*, vol. 121, no. 17, pp. 2900–2908, Sep. 2015, doi: 10.1002/CNCR.29475.
37. A. Stengel *et al.*, "Number of RUNX1 mutations, wild-type allele loss and additional mutations impact on prognosis in adult RUNX1-mutated AML," *Leukemia*, vol. 32, no. 2, pp. 295–302, Feb. 2018, doi: 10.1038/LEU.2017.239.
38. G. A. Toruner *et al.*, "Clinical Utility of Optical Genome Mapping as an Additional Tool in a Standard Cytogenetic Workup in Hematological Malignancies," *Cancers (Basel).*, vol. 17, no. 9, May 2025, doi: 10.3390/CANCERS17091436.
39. Y. M. N. Akkari *et al.*, "Evidence-based review of genomic aberrations in B-lymphoblastic leukemia/lymphoma: Report from the cancer genomics consortium working group for lymphoblastic leukemia," *Cancer Genet.*, vol. 243, pp. 52–72, May 2020, doi: 10.1016/j.cancergen.2020.03.001.
40. K. M. Schieffer *et al.*, "Points to consider for the next-generation-sequencing-based detection of copy-number abnormalities (CNAs) and balanced chromosomal rearrangements in neoplastic disorders: A

 doi:10.20944/preprints202605.0494.v1

statement of the American College of Medical Genetics and Genomics (ACMG).," *Genet. Med.*, vol. 28, no. 3, p. 101658, Jan. 2026, doi: 10.1016/j.gim.2025.101658.

41. Á. Díaz-González *et al.*, "Copy-Neutral Loss of Heterozygosity in Myelofibrosis," *Journal of Molecular Diagnostics*, vol. 28, no. 4, Apr. 2026, doi: 10.1016/j.jmoldx.2025.12.006.